To cite this version :

Original article

Combined 3D analysis of lower-limb morphology and function in children with idiopathic equinovarus clubfoot: A preliminary study

Virginie Rampal [a,b,*], Pierre-Yves Rohan [a], Helene Pillet [a], Aurore Bonnet-Lebrun [a],
Mickael Fonseca [a], Eric Desailly [d], Philippe Wicart [c], Wafa Skalli [a]

[a] Institut de biomécanique humaine Georges-Charpak, Arts et Métiers ParisTech, 75013 Paris, France
[b] Service d'orthopédie infantile, hôpitaux pédiatriques de Nice, CHU Lenval, 06000 Nice, France
[c] Service d'orthopédie infantile, hôpital Necker–Enfants-Malades, 75015 Paris, France
[d] Unité d'analyse du mouvement, pôle recherche et innovation, fondation Ellen-Poidatz, 77310 Saint-Fargeau-Ponthierry, France

ABSTRACT

Keywords:
Child lower limb
Equinovarus clubfoot
Gait analysis
Biplanar radiography
Feasibility

Introduction: In children treated for idiopathic equinovarus clubfoot (EVCF), the relation between morphologic defects on clinical examination and standard X-ray on the one hand and functional abnormalities on the other is difficult to objectify. The aim of the present study was to demonstrate the feasibility of combined 3D analysis of the foot and lower limb based on biplanar EOS radiographs and gait analysis. The study hypothesis was that this provides better understanding of abnormalities in form and function.
Methods: Ten children with unilateral EVCF and "very good" clinical results were included. They underwent gait analysis on the Rizzoli Institute multisegment foot model. Kinematic data were collected for the hip, knee, ankle and foot (hindfoot/midfoot, midfoot/forefoot and hindfoot/forefoot). Biplanar EOS radiographs were taken to determine anatomic landmarks and radiological parameters.
Results: Complete acquisition time was around 2 hours per patient. No significant differences were found between EVCF and healthy feet except for calcaneal incidence, tibiocalcaneal angle and hindfoot/midfoot and hindfoot/forefoot inversion.
Discussion: The feasibility of the combined analysis was confirmed. There were no differences in range of motion, moment or power between EVCF and healthy feet in this series of patients with very good results. The functional results are related to radiological results within the normal range. The protocol provided anatomic and kinematic reference data. A larger-scale study could more objectively assess the contribution of EOS radiography using optoelectronic markers.
Level of evidence: II, low-power prospective study.

1. Introduction

Children treated for equinovarus clubfoot (EVCF) during growth are followed up in consultation on clinical examination [1,2] and standard 2D X-ray, which is insufficient for fine analysis of defects and for complete assessment [3–6]. A 3D weight-bearing foot reconstruction technique based on biplanar radiographs was recently described [7,8], and pediatric reference values have been reported [8]. The model [9] can also locate joint rotation centers with respect to the optoelectronic markers used in quantified analysis of movement (QAM) [10,11]. Radiographs, however, correlate poorly with function, and QAM is a complementary assessment instrument. Given the small size of children's feet, QAM treats the foot as a rigid segment, neglecting motion between the hind-, mid- and fore-foot [12]. The Rizzoli Institute multisegment model [13] describes inter-segment motion and is able to analyze such abnormalities [14].

Associating 3D reconstruction to QAM could improve decision-making in children with EVCF, by providing global analysis relating form to function.

The aim of the present preliminary study was to assess the feasibility of combing QAM on a multisegment model to 3D radiology based on biplanar imaging, to improve assessment of EVCF. The study hypothesis was that this improves understanding of lower-limb abnormalities.

* Corresponding author.
  E-mail address: rocher-rampal.v@pediatrie-chulenval-nice.fr (V. Rampal).

2. Material and method

2.1. Patients

After securing review board approval (CPP NX06036), 10 patients (9 boys, 1 girl) aged 7–11 years were included during pediatric orthopedics outpatient consultation, with consent form signed by parents and children. They were being followed for unilateral EVCF treated functionally since the first week of life. Pathological feet formed the EVCF group, with contralateral feet as controls.

2.2. Method

QAM was performed in the Georges Charpak Human Biomechanics Institute of Paris (France) on an optoelectronic analysis system comprising 12 video-cameras (Vicon Motion System Ltd., Oxford Metrics, UK) and 4 synchronized force platforms (Advanced Mechanical Technology Inc., Watertown, MA, USA). The optoelectronic markers were positioned following the Rizzoli Institute method [13]. Biplanar radiographs were taken using the EOS system (EOS Imaging, France).

2.3. Measurement protocol

2.3.1. Clinical assessment

Feet were assessed by an orthopedic surgeon following Ghanem and Seringe [15].

2.3.2. Subject preparation

The optoelectronic markers were positioned following the Rizzoli Institute protocol [13] by the orthopedic surgeon, trained in the method. Markers were 9-mm diameter (Fig. 1a and b), except on the foot, where 2-mm minimarkers were used (Fig. 1c and d).

2.3.3. EOS imaging

Biplanar radiographs were acquired with the markers in position, in 3 modes per subject: standardized free-standing [16] (Fig. 1a), and right and left monopodal weight-bearing with contralateral foot in equinus [8] (Fig. 1b). AP and lateral views were taken each time (Fig. 1c and d).

2.3.4. Static calibration

Ahead of gait trials, the minimarkers were replaced by standard 9-mm markers (Fig. 1e) for static calibration.

2.3.5. Gait analysis

Subjects walked barefoot at spontaneous speed for about 5 m. The test was concluded after 5 validated trials.

2.4. Data processing

2.4.1. 3D reconstructions and radiologic parameters

3D reconstruction was performed by a trained clinician [17,18]. For feet, reconstruction followed the previously described method [10]. In patients 1 to 5, reconstruction was repeated 3 times, to test intra-operator reproducibility.

Table 1 and Fig. 2 show the radiological parameters.

2.4.2. Gait analysis

Reference planes were determined following the Rizzoli Institute model [13]: flexion/extension (Flex/Ext), internal/external rotation (Int/Ext), abduction/adduction (Abd/Add) and, for the ankle, dorsiflexion/plantar flexion (Dors/Plan), inversion/eversion (Inv/Ev) and abduction/adduction (Abd/Add).

Rotations were calculated: pelvis-femur, calf-hindfoot (ankle), hind-midfoot (Cal-Mid), mid-forefoot (Mid-Met), and hind-midfoot (Cal-Met). The mean angle over all trials was used for calculation. Scatter was calculated as standard deviation. Ground reaction force, kinematics and joint moment were also calculated.
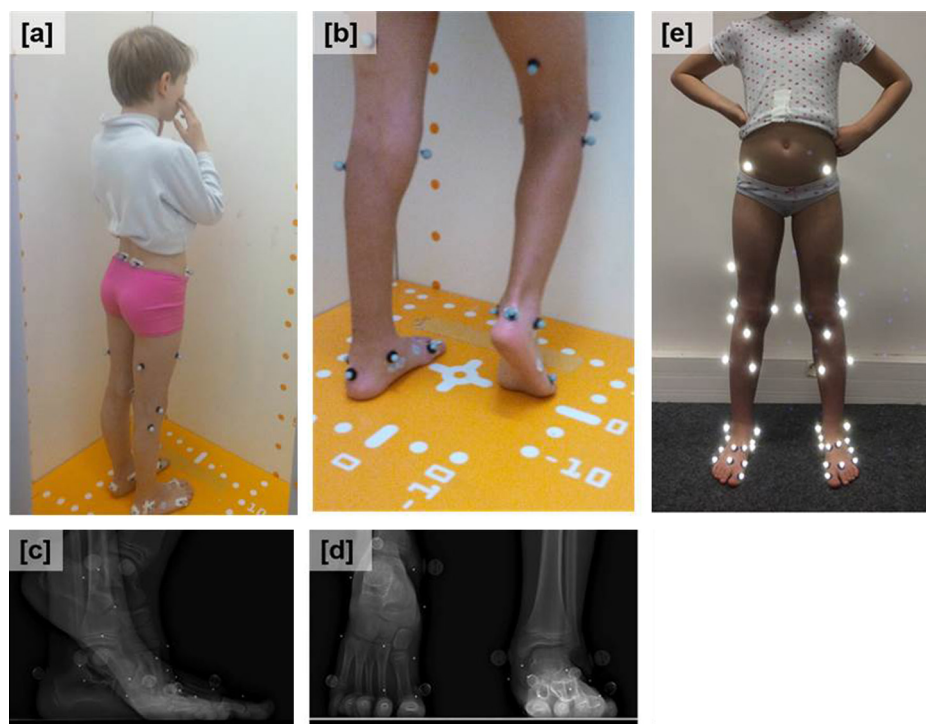

Fig. 1. Markers positioned according to the Rizzoli Institute multisegment protocol [13]: a: standardized free-standing position in EOS system; b: monopodal position and contralateral equinus; c: AP view; d: sagittal view; e: optoelectronic markers (9 mm).

Table 1

Radiology results and reference values in the literature: femorotibial angle (FTA), femoral head diameter (FHD), neck-shaft angle (NSA), mechanical femoral angle (MFA), mechanical tibial angle (MTA), hip-knee-shaft angle (HKS), femur/tibia ratio (F/T), femoral torsion (FT), tibial torsion (TT), calcaneal incidence (CI), talo-calcaneal divergence (TCD), tibiotalar angle (TTA), tibiocalcaneal angle (TCA), talonavicular cover angle (TNCA), Méary angle, 1st metatarsal incidence angle (M1IA). NR: non-reproducible; n/a: not applicable.

Parameter	Pathologic side	Healthy side	Reference values
Pelvis			
Sacral slope (°) [20]	40 ± 8	n/a	38 ± 8
Pelvic tilt (°) [20]	3 ± 9	n/a	6 ± 7
Pelvic incidence (°) [20]	45 ± 8	n/a	45 ± 9
Lower limb			
HKS (°) [21]	5 ± 1	4 ± 1	7 ± 5
FTA (°) [21]	178 ± 2	177 ± 1	179 ± 3
FHD (mm) [21]	35 ± 2	34 ± 2	34 ± 3
NSA (°) [21]	142 ± 7	137 ± 8	131 ± 6
MTA (°) [21]	88 ± 1	89 ± 2	89 ± 3
MFA (°) [21]	93 ± 1	92 ± 2	3 ± 3
Neck length (mm) [21]	36 ± 4	41 ± 5	n/a
F/T [21]	1 ± 0	1 ± 0	1 ± 0
FT (°) [21]	25 ± 9	25 ± 12	n/a
TT (°) [21]	27 ± 23	27 ± 26	n/a
Foot			
CI (°) [8]	12 ± 5	19 ± 6	20 [14; 34]
TCA (°) [8]	75 ± 4	65 ± 5	67 [54; 77]
TTA (°) [8]	-4 ± 6	-4 ± 3	0 [−10; 7]
TCD (°) [8]	NR	NR	[35–50]
TNCA (°) [8]	NR	NR	[5–39]
Méary angle (°) [8]	NR	NR	[0–15]
M1IA (°) [8]	20 ± 5	20 ± 4	21 [15; 30]

Pelvic and lower-limb values are reported as mean ± Standard Deviation (SD); foot values are reported as mean ± SD with reference values as mean ± range.

2.5. Statistics

2.5.1. Measurement uncertainty

Given the small size of children's feet and the large number of markers needed for gait analysis, analysis was performed in 2 healthy subjects (aged 8 and 10 years) to assess the reproducibility of marker positioning. Inter-trial and inter-session variation was assessed.

The impact of marker positioning uncertainty on gait parameters was quantified on the Monte Carlo method [19].

2.5.2. Statistical analysis

The Wilcoxon signed ranks test was used for inter-group comparisons. The significance threshold was set at $p < 0.05$.

3. Results

3.1. Demographics and clinical assessment

Mean age was 9.2 years (range, 7–11 years). All feet showed very good results: Ghanem-Seringe score, 88–100 [15].

3.2. Radiologic results

Table 1 shows radiologic results. Four foot parameters showed $< 3°$ reproducibility: tibiocalcaneal angle, calcaneal incidence, tibiotalar angle, and 1st metatarsal incidence. There were significant inter-group differences in calcaneal incidence and tibiocalcaneal angle.

3.3. Gait analysis

Measurement uncertainty was $< 4°$. Table 2 shows the main angles (Dors/Plan, Inv/Ev). There were no significant inter-group differences except for hindfoot-midfoot inversion ($p = 0.04$) and hindfoot-forefoot inversion ($p = 0.01$) (Fig. 3).

Table 3 shows kinetic results. There were no significant inter-group differences.

4. Discussion

There are few elements describing the relations between foot architecture, kinematics and gait kinetics in children with EVCF;
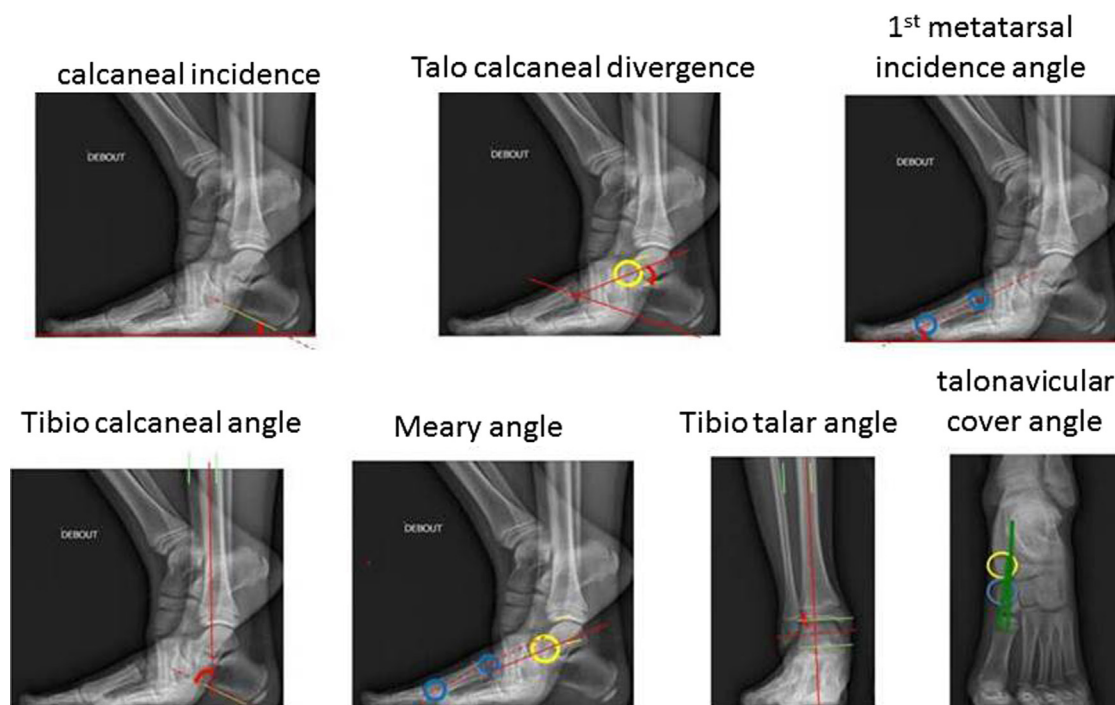

Fig. 2. Radiologic parameters of foot.

Table 2
Kinematic results in EVCF and controls (mean ± SD).

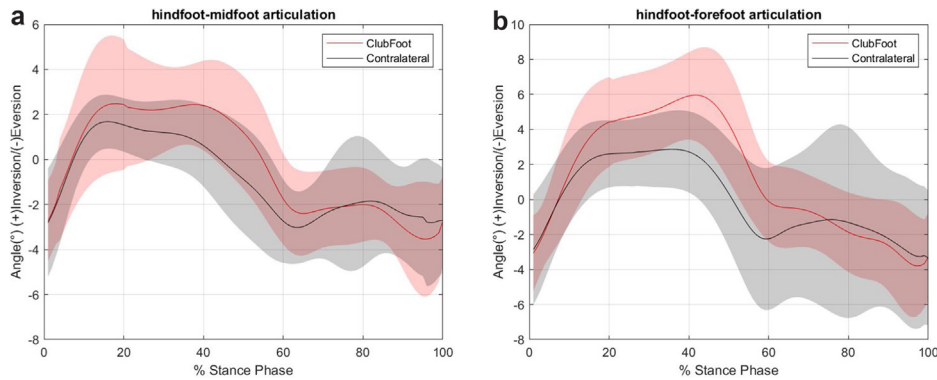| Joint	Dorsiflexion (°)		Plantar flexion (°)		Inversion (°)		Eversion (°)	
	EVCF	Control	EVCF	Control	EVCF	Control	EVCF	Control
Ankle	9.0 ± 6.7	10.4 ± 4.6	10.0 ± 4.8	11.4 ± 3.6	6.4 ± 3.0	5.1 ± 3.4	8.7 ± 4.4	5.9 ± 4.0
Hind/midfoot	5.6 ± 3.4	4.8 ± 2.2	5.2 ± 2.6	6.3 ± 2.2	3.6 ± 2.8	2.0 ± 1.2	4.3 ± 1.9	4.1 ± 1.8
Mid/forefoot	2.8 ± 1.0	2.3 ± 1.3	4.0 ± 2.0	5.4 ± 2.5	3.0 ± 1.5	3.1 ± 2.4	2.3 ± 1.6	1.9 ± 2.1
Hind/forefoot	7.5 ± 2.4	6.7 ± 2.3	7.3 ± 3.7	11.5 ± 3.0	6.4 ± 2.6	3.4 ± 2.0	4.5 ± 2.2	4.5 ± 2.5

Fig. 3. Mean inversion/eversion in (a) hind/midfoot, (b) hind/forefoot.

Table 3
Kinetic and ground reaction force results in EVCF and controls (mean ± SD).

	EVCF	Control
	12.2 ± 2.3	11.2 ± 1.7
Vertical force at heel contact (N/kg)	10.5 ± 0.87	10.2 ± 2.1
Vertical force at propulsion (N/kg)	1.9 ± 0.3	1.9 ± 0.4
Anterior force (N/kg)	1.9 ± 0.4	2.0 ± 0.5
Posterior force (N/kg)	1.8 ± 0.7	1.6 ± 0.5
Ankle plantar flexion moment (N.m/kg)	4.5 ± 2.0	5.3 ± 2.8

Standard assessment is based on clinical examination and 2D radiography. Although QAM is a promising means of assessment, gait laboratory data are insufficient for clinical decision-making. The present study had the interest of performing the first combined analysis associating 3D reconstruction of the foot and lower limb from biplanar radiographs to QAM using a multisegment foot model. The feasibility of the protocol in a clinical setting (test time, 2 hours), differentiating hind-, fore- and mid-foot, was confirmed. The study cannot be a basis for a novel decision-tree in EVCF, (1) because sample size was small, and (2) as subjects had exclusively very good results. It does, however, open the way for a larger-scale exploration to enhance decision-making.

The EVCF group showed no particular 3D morphologic abnormalities [20,21] or gait-related abnormalities, in contrast to the literature for pathologic children [22–24]. However, the good results underlying the present series were the main study limitation, precluding correlation analysis of defects. Future studies should explore the methodology proposed for more severe pathologies.

On 3D radiology, only 4 foot parameters were reproducible (95% CI, <3°), due to the difficulty of visualizing the hindfoot [8]. This might be resolved by different foot positioning during acquisition. The difference in calcaneal incidence was related to lower ankle dorsiflexion in the EVCF group.

Positioning a large number of markers on a child's foot was not a technical problem, and applying the Rizzoli multisegment model [13] was feasible. We found no intergroup differences in kinematics or kinetics, unlike in other reports [25,26], and the results matched those for healthy children in the sole publication to report them [14]. There was, however, a difference in hindfoot/midfoot and midfoot/hind- and fore-foot motion, confirming that models representing the foot as a single segment are inadequate for describing abnormalities [27].

In this study, biplanar radiographs were taken with markers in position. This is clinically demanding, and presupposes a single site for QAM and biplanar radiography, but enables more precise determination of anatomic landmarks. The number of patients included was insufficient for conclusions to be drawn. Even so, as seen in Fig. 4, the interpretation of movement can differ considerably according to the landmark, and a larger-scale study is needed to
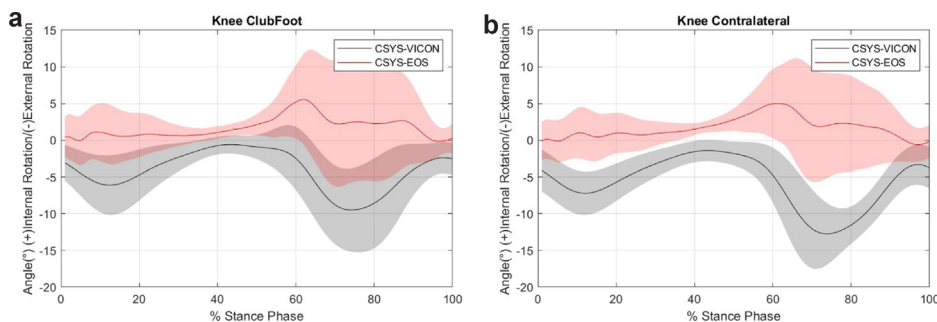

Fig. 4. Mean internal/external rotation in (a) EVCF (left) and (b) controls (right). Gray curve: landmarks based on optoelectronic markers; red curve: landmarks based on EOS radiographs.

determine more objectively the contribution if any of EOS radiography with optoelectronic markers in position.

The present preliminary study focused exclusively on EVCF, but could be extended to other pathologies, to enhance understanding, help diagnosis and improve treatment in lower-limb pathology. Notably, the QAM protocol of the Rizzoli Institute [13] is contributive in case of clinical suspicion of specifically midfoot abnormality.

Disclosure of interest

Funding

Author contributions

V. Rampal: protocol, inclusion, data acquisition and processing, article writing.

P.Y. Rohan, H. Pillet, A. Bonnet Lebrun: data processing and analysis.

M. Fonseca, E. Desailly: gait analysis protocol and acquisition.

P. Wicart: inclusion, marker positioning, data analysis, re-editing.

W. Skalli: data analysis, re-editing.

References

[1] Sawatzky B, Sanderson D, Beauchamp R, Outerbridge A. Ground reaction forces in gait in children with clubfeet — A preliminary study. Gait Posture 1994;2:123–7.

[2] Schleicher I, Lappas K, Klein H, Szalay G, Kordelle J. Follow up of complete subtalar release for clubfoot — Evolution of different scores. Foot Ankle Surg 2012;18:55–61.

[3] Cooper DM, Dietz FR. Treatment of idiopathic clubfoot. A thirty-year follow-up note. J Bone Joint Surg 1995;77:1477–89.

[4] Laaveg S, Ponseti I. Long-term results of treatment of congenital club foot. J Bone Joint Surg 1980;62:23–31.

[5] Lau JH, Meyer LC, Lau HC. Results of surgical treatment of talipes equinovarus congenita. Clin Orthop Rel Res 1989:219–26.

[6] Prasad P, Sen RK, Gill SS, Wardak E, Saini R. Clinico-radiological assessment and their correlation in clubfeet treated with postero-medial soft-tissue release. Int Orthop (SICOT) 2009;33:225–9.

[7] Rohan P-Y, Perrier A, Ramanoudjame M, Hausselle J, Lelièvre H, Seringe R, et al. Three-dimensional reconstruction of foot in the weightbearing position from biplanar radiographs: evaluation of accuracy and reliability. J Foot Ankle Surg 2018;57:931–7.

[8] Rampal V, Rohan P-Y, Saksik R, Wicart P, Skalli W. Assessing 3D paediatric foot morphology using low-dose biplanar radiography: parameter reproducibility and preliminary values. Orthop Traumatol Surg Res 2018;104: 1083–9.

[9] Dubousset J, Charpak G, Dorion I, Skalli W, Lavaste F, Deguise J, et al. A new 2D and 3D imaging approach to musculoskeletal physiology and pathology with low-dose radiation and the standing position: the EOS system. Bull Acad Natl Med 2005;189:287–97 [discussion 297–300].

[10] Pillet H, Sangeux M, Hausselle J, El Rachkidi R, Skalli W. A reference method for the evaluation of femoral head joint center location technique based on external markers. Gait Posture 2014;39:655–8.

[11] Sangeux M, Pillet H, Skalli W. Which method of hip joint centre localisation should be used in gait analysis? Gait Posture 2014;40:20–5.

[12] MacWilliams BA, Cowley M, Nicholson DE. Foot kinematics and kinetics during adolescent gait. Gait Posture 2003;17:214–24.

[13] Leardini A, Benedetti MG, Berti L, Bettinelli D, Nativo R, Giannini S. Rear-foot, mid-foot and fore-foot motion during the stance phase of gait. Gait Posture 2007;25:453–62.

[14] Deschamps K, Staes F, Roosen P, Nobels F, Desloovere K, Bruyninckx H, et al. Body of evidence supporting the clinical use of 3D multisegment foot models: a systematic review. Gait Posture 2011;33:338–49.

[15] Ghanem I, Seringe R. Comparaison des méthodes d'évaluation des résultats du traitement du pied bot varus équin congénital. Rev Chir Orthop Trauma 1995;81:616–21.

[16] Faro FD, Marks MC, Pawelek J, Newton PO. Evaluation of a functional position for lateral radiograph acquisition in adolescent idiopathic scoliosis. Spine 2004;29:2284–9.

[17] Chaibi Y, Cresson T, Aubert B, Hausselle J, Neyret P, Hauger O, et al. Fast 3D reconstruction of the lower limb using a parametric model and statistical inferences and clinical measurements calculation from biplanar X-rays. Comput Methods Biomech Biomed Engin 2012;15:457–66.

[18] Mitton D, Deschênes S, Laporte S, Godbout B, Bertrand S, Guise JA, et al. 3D reconstruction of the pelvis from bi-planar radiography. Comput Methods Biomech Biomed Engin 2006;9:1–5.

[19] Chib S. Monte Carlo methods and Bayesian computation: overview. Int Encyclopedia Soc Behav Sci 2001:10004–9.

[20] Guigui P, Levassor N, Rillardon L, Wodecki P, Cardinne L. Physiological value of pelvic and spinal parameters of sagittal balance: analysis of 250 healthy volunteers. Rev Chir Orthop Reparatrice Appar Mot 2003;89:496–506.

[21] Rampal V, Rohan P-Y, Assi A, Ghanem I, Rosello O, Simon A-L, et al. Lower-limb lengths and angles in children older than six years: reliability and reference values by EOS® stereoradiography. Orthop Traumatol Surg Res 2018;104: 389–95.

[22] Bailly R, Lempereur M, Pons C, Houx L, Thepaut M, Borotikar B, et al. 3-D lower extremity bone morphology in ambulant children with cerebral palsy and its relation to gait. Ann Phys Rehabil Med 2019, http://dx.doi.org/10.1016/j.rehab.2019.03.001 [pii: S1877-0657(19)30037-5. Epub ahead of print].

[23] Buldt AK, Murley GS, Butterworth P, Levinger P, Menz HB, Landorf KB. The relationship between foot posture and lower limb kinematics during walking: a systematic review. Gait Posture 2013;38:363–72.

[24] Shin HS, Lee JH, Kim EJ, Kyung MG, Yoo HJ, Lee DY. Flatfoot deformity affected the kinematics of the foot and ankle in proportion to the severity of deformity. Gait Posture 2019;72:123–8.

[25] El-Hawary R, Karol L, Jeans K, Richards B. Gait analysis of children treated for clubfoot with physical therapy or the Ponseti Cast Technique. J Bone Joint Surg 2008;90:1508–16.

[26] Karol LA, Jeans K, ElHawary R. Gait analysis after initial nonoperative treatment for clubfeet: intermediate term follow-up at age 5. Clin Orthop Relat Res 2009;467:1206–13.

[27] Eerdekens M, Staes F, Matricali GA, Wuite S, Peerlinck K, Deschamps K. Quantifying clinical misinterpretations associated to one-segment kinetic foot modelling in both a healthy and patient population. Clin Biomech (Bristol, Avon) 2019;67:160–5.